RSC Advances

PAPER

View Article Online
View Journal | View Issue

Cite this: *RSC Adv.*, 2020, **10**, 3529

Tuning the gradient structure of highly breathable, permeable, directional water transport in bi-layered Janus fibrous membranes using electrospinning

Yue Zhang,†[a] Ting-Ting Li,†[abc] Hai-Tao Ren,[a] Fei Sun,[a] Qi Lin,*[de] Jia-Horng Lin *[abcfgh] and Ching-Wen Lou*[acdgij]

Received 3rd August 2019
Accepted 5th December 2019

DOI: 10.1039/c9ra06022g

rsc.li/rsc-advances

In this paper, a novel bi-layered Janus fibrous electrospun membrane with robust moisture permeable, breathable and directional water transport properties is successfully fabricated and reported for the first time. This fibrous membrane consists of a thin inner layer of hydrophobic thermoplastic polyurethane (TPU) and a thick outer layer of super hydrophilic polyacrylonitrile (PAN). The PAN layer is coated with dopamine (PDA) to tailor the wettability. The subsequent TPU–PAN/PDA membrane demonstrates outstanding wettability and thickness gradients, which facilitate directional water transport from the TPU to the PAN/PDA layer and improve the WVT rate to 9065 g m^{-2} d^{-1} and the air permeability to 100 mm s^{-1} (5.0 times higher than a commercial membrane). Furthermore, a plausible mechanism explaining the bi-layered Janus fibrous membrane performance is studied. The fibrous membrane is suggested to be a promising candidate for various applications, especially in moisture-wicking clothing.

1. Introduction

Directional water transport is a predominant property of functional textiles used in daily life against continuous sweat release.[1,2] The growing demand for quick drying performance has driven researchers to devote continuous efforts toward improving the directional water transfer properties of textiles. Directional water transport materials can be categorized into two major types according to the wettability profile, namely those with a wettability gradient and those with Janus wettability. Traditional directional water transport textiles include single-layered wettability gradient textiles and double-layered Janus wettability microfiber- or nanofiber-based textiles.[3–8] All these textiles have their own advantages. Compared with wettability gradient textiles, double-layered Janus wettability microfiber- or nanofiber-based textiles have great potential for achieving better directional water transport properties because Janus membranes have layers with opposite wettability: a hydrophobic inner layer that ensures low water absorption, and a hydrophilic outer layer that draws sweat out from the hydrophobic side and transports it to the hydrophilic side. Owing to their remarkable advantages, which also include simple preparation processes and the individual and facile tailoring of wettability, various high-performance directional water transport bi-layered Janus membrane nanofibers have been processed *via* electrospinning and they have been widely applied in sportswear, work-wear, and military uniforms.[9–12] For example, Dong *et al.*[3] prepared a bi-layered nanofibrous membrane containing polyacrylonitrile (PAN)-PVDF (core–shell) and cellulose acetate; additionally, they developed bi-layered polystyrene/polyacrylonitrile electrospun membranes that exhibited effective one-way transport properties.[4] Cao *et al.*[13] created tri-layered fibrous membranes consisting of polyacrylonitrile (PAN–SiO_2) fibers, and polyurethane–polyacrylonitrile (PU–PAN) fibers in combination with polyurethane (PU) fibers; the PU–PAN fiber transfer layer could continuously and spontaneously guide the directional water transport and

[a]*Innovation Platform of Intelligent and Energy-Saving Textiles, School of Textile Science and Engineering, Tiangong University, Tianjin 300387, China. E-mail: jhlin@fcu.edu.tw*

[b]*Tianjin and Ministry of Education Key Laboratory for Advanced Textile Composite Materials, Tiangong University, Tianjin 300387, China*

[c]*Fujian Key Laboratory of Novel Functional Fibers and Materials, Minjiang University, Fuzhou 350108, China*

[d]*Ocean College, Minjiang University, Fuzhou 350108, China. E-mail: linqi@mju.edu.cn*

[e]*Fujian Engineering Research Center of New Chinese Lacquer Material, Minjiang University, Fuzhou 350108, China*

[f]*Laboratory of Fiber Application and Manufacturing, Department of Fiber and Composite Materials, Feng Chia University, Taichung 40724, Taiwan*

[g]*College of Textile and Clothing, Qingdao University, Shandong 266071, China*

[h]*Department of Fashion Design, Asia University, Taichung 41354, Taiwan*

[i]*Department of Medical Research, China Medical University Hospital, China Medical University, Taichung 40402, Taiwan*

[j]*Department of Bioinformatics and Medical Engineering, Asia University, Taichung 41354, Taiwan. E-mail: cwlou@asia.edu.tw*

† These authors contributed equally to this work.

thus prevent skin from being rewetted. Wang *et al.*[14] studied the feasibility of preparing an antigravity directional water transport polylactic acid/cellulose/polyurethane acetate (PLA/CA/PU) electrospun composite membrane. Wu *et al.*[15] designed and prepared a heterogeneous and seamless coupling polyurethane/crosslinked poly(vinyl alcohol) (PU/c-PVA) fibrous Janus composite membrane with wettability properties. Xu *et al.*[16,17] presented a facile tunable method and design guidelines to prepare a series of Janus membranes consisting of negatively or positively charged nanofillers to enrich the number of potential applications.

From a comfort perspective, people need to maintain a comfortable microclimate when working or exercising under special circumstances. In addition to good directional water transport properties, the moisture permeability and breathability of textiles are also of immense importance. To provide insight into obtaining comfortable performance, we have evaluated the moisture permeable and breathable properties of Janus membranes. Previous literature studies have reported various designs for directional water transport Janus fibrous membranes using electrospinning methods. Unfortunately, few studies have been conducted relating to directional water transport in functional and comfortable materials from the perspective of moisture permeability and breathability properties. Ju *et al.* in 2017 (ref. 18) were the first to fabricate directional water transport, moisture-permeable, and breathable thermoplastic polyurethane (TPU)/TPU-TBAC dual-layer electrospun membranes. However, the membranes exhibited limited moisture permeability of 2170 g m^{-2} d^{-1} and low breathability of 1.16 mm s^{-1}. Further investigations were carried out through changing the materials and tailoring the thickness gradient, which increased the moisture permeability to 12 110 g m^{-2} d^{-1}, but no evaluation of the breathability was performed.[19]

To prepare Janus fibrous membranes with improved moisture permeability, breathability and bi-layered directional water transport properties, a composite material composed of at least two heterogeneous layers with different performances is needed. In this study, a TPU–PAN/PDA bi-layered Janus fibrous membrane is fabricated for the first time. TPU is frequently used in PU family moisture permeable and breathable textile substrates, and it is chosen as the inner layer. PDA, which is rich in hydrophilic groups, is often employed as a modifier to improve the hydrophilicity and reactivity of substrates such as polystyrene nanofibers,[4,20] polytetrafluoroethene,[21] clay,[22] and even anodic aluminum oxide.[23] In the present study, PDA is used to tailor the surface hydrophilicity of the PAN outer layer because PDA can be facilely coated onto nanofibers *via in situ* polymerization.[20] Our work focuses on designing a bi-layered Janus fibrous membrane that combines asymmetric thickness and surface energy gradients and offers ample opportunities to achieve the excellent moisture permeable and breathable performance of "push–pull effect" directional water transport textiles. The morphology, surface chemistry structure, wetting behavior, moisture permeable properties and breathability of the superhydrophilic fibrous membrane are presented in this paper. Moreover, the effectiveness of our asymmetric thickness gradient and surface energy gradient design in providing moisture permeable, breathable, and directional water transport properties in bi-layered Janus fibrous membranes is demonstrated.

2. Experimental

2.1 Materials

The polymer TPU (Tecoflex EG-93A) was purchased from Lubrizol Corporation (Wickliffe, Ohio, USA). *N*,*N*-Dimethylformamide (DMF) and LiCl were obtained from Tianjin Kermel Chemical Reagent Co., Ltd, China. Dopamine (PDA), and tris(hydroxymethyl)aminomethane (Tris) were provided by Adamas Reagent Co., Ltd, Switzerland. Polyacrylonitrile powder (PAN, average M_w = 90 000) was provided by Spectrum Chemical Manufacturing Corp., California, USA. Distilled water was used in this work.

2.2 Preparation of TPU and PAN nanofibers

The polymer solutions were prepared by dissolving TPU in LiCl/DMF ionic solution under vigorous magnetic stirring at ambient temperature for 12 h using a standard electrospinning machine. The TPU concentration was kept at 18 wt% in all solutions, while the LiCl concentration remained at 0.007 wt%. Then, the TPU solution was pumped at a fixed rate of 0.8 mL h^{-1} using a working voltage of 45 kV. The PAN solution was prepared by dissolving PAN (3.6 g) in DMF (26.4 g) solution under continuous stirring to ensure complete dissolution. The fixed flow rate and direct current voltage were 0.8 mL h^{-1} and 20 kV, respectively. The distance between the needle tip and the collector was maintained at 15 cm. Afterwards, the obtained membrane was vacuum-dried at 70 °C for 2 h.

2.3 Preparation of single-layer PAN/PDA

Dip-coating surface modification was applied to construct the super hydrophilic nanofibrous layer. First, 0.12 g of Tris–HCI and 0.20 g of dopamine were dissolved in 100 mL of distilled water to prepare 2 mg mL^{-1} dopamine solution. PAN nanofibrous membranes treated with plasma enhancement were immersed in the dopamine solution for various treatment times of 0, 3, 6, and 12 h. Subsequently, the coated membranes were dried at 70 °C for 24 h in a laboratory dryer under hot air circulation.

2.4 Preparation of bi-layered TPU–PAN/PDA Janus fibrous membranes

In our study, two criteria are required during the design of Janus fibrous membranes: (i) the Janus fibrous membranes must enable directional water transport based on different surface energy gradients; and (ii) the membrane should be sufficiently thin to obtain an outstanding WVT rate and breathability through the porous matrix. Fig. 1 shows the preparation process for the bi-layered Janus fibrous membranes. First, the obtained PAN fibrous membranes were activated using an oxygen plasma enhancement machine (TS-10MT) from Shen Zhen Dongxin Plasma Technology. The operating power and treatment time

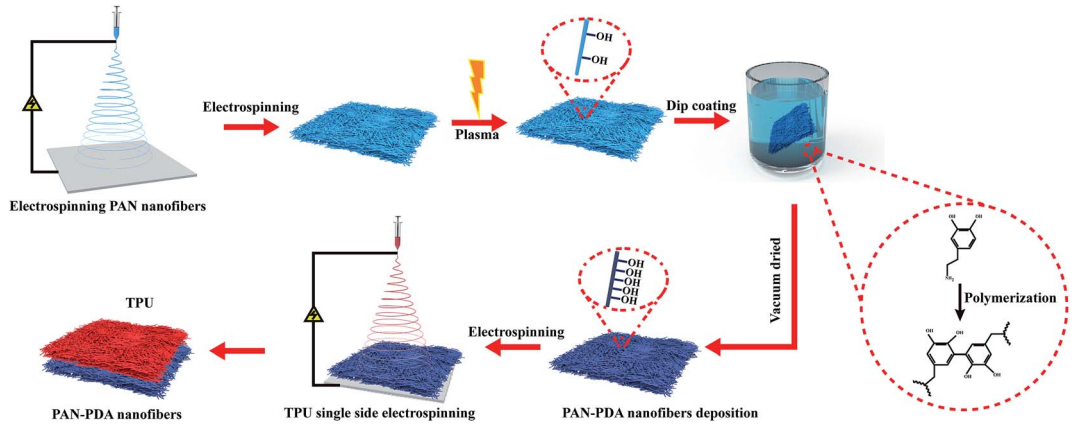

Fig. 1 Preparation process for the bi-layered Janus fibrous membranes.

were controlled at 100 W and 100 s, respectively. Second, a super hydrophilic membrane with a wider wetting area was designed after PDA dip-coating treatment. Third, bi-layered TPU–PAN/PDA Janus fibrous membranes were obtained *via* the electrospinning of the TPU/DMF solution on one side of the super hydrophilic fibrous membrane. The obtained bi-layered TPU–PAN/PDA Janus fibrous membranes are denoted as PAN-FM-*y*-TPU (*y* is 15, 30, 45, or 60 depending on the PAN spinning time). In addition, the TPU–PAN/PDA fibrous membranes are denoted as PAN-NF-30-TPU-*y* (*y* is 0, 2, or 3 depending on the various TPU spinning time: 0 represents 4 min, 2 represents 8 min, and 3 represents 12 min). Finally, the baking temperature and time for the obtained fibrous membranes were 70 °C and 2 h, respectively.

2.5 Measurements and characterization

Field emission scanning electron microscopy (SEM, TM3030, HITACHI, Tokyo, Japan) was used to measure the morphologies of the fibrous membranes. The surface chemistry structure was analyzed using a FT-IR spectrometer (NICOLET iS10, Thermo Fisher Scientific, US). Wicking height tests were carried out as specified in the AATCC TM 197 standard. Each sample had a specified size of 200 mm × 25 mm, then rhodamine B was added into the distilled water to track the movement of the water. According to GB/T 21655.1-2008, the water evaporation rate and water absorption data were measured. The membranes were dropped into 0.2 g of distilled water, and then their weights were measured every 5 min. In the water absorption tests, samples with a size of 100 mm × 100 mm were soaked in distilled water and dried at room temperature until no water leaked from them; then, their weights were measured. The wettability testing of the membranes was conducted using a surface contact angle instrument (JC2000DM, Shanghai Zhongchen Digital Testers, Shanghai, China). The water transport behavior of the samples was tested using a moisture management tester (MMT, SDL ATLAS). The WVT rates were evaluated according to the ASTM E96-$CaCl_2$ standard desiccant method, using a water vapor transmission tester (YG501D testing chamber, Wenzhou Fangyuan Instrument Co., Ltd, China); the testing was conducted in a test chamber at 23 °C and 90% RH. The air permeability of the samples was measured using an automatic air permeability instrument (YG 461E testing chamber, Wenzhou Fangyuan Instrument Co., Ltd, China).

3. Results and discussion

3.1 Morphologies, surface chemistry structures and wetting behaviors of the super hydrophilic fibrous membranes

Fig. 2a–c shows SEM images of the pristine TPU, PAN, and PAN/PDA fibrous membranes used in this work, respectively. Fig. 2d and 3 present the surface chemistry structures and wetting behaviors of the PAN/PDA fibrous membranes with respect to the PDA treatment time. As presented in Fig. 2a and b, the pristine TPU and PAN fibrous membranes exhibit uneven morphology features. The super hydrophilic fibrous membrane is obtained *via* introducing a PDA layer onto the PAN surface.[20–23] Fig. 2c clearly demonstrates that PDA is well deposited onto the surface of the PAN nanofibers owing to DA self-polymerization.[24,25] This result is confirmed from the FT-IR spectra. As shown in Fig. 2d, all the spectra display a characteristic PAN peak at 2230 cm^{-1} from the stretching vibration of the nitrile group (–CN). However, this characteristic peak at 2230 cm^{-1} decreased after the PAN was coated with PDA, an outcome that may be attributed to the nanofibers being covered with PDA. Meanwhile, the peaks related to the –OH stretching and C–O vibrations of phenolic moieties in the spectra became gradually stronger and could be seen at approximately 3300 and 1260 cm^{-1}, respectively, indicating an increased concentration of PDA.[4,24]

To study the wetting behaviors of the nanofibrous membranes, wicking height, water evaporation rate, water absorption, and water contact angle measurements were carried out at different treatment times, as shown in Fig. 3a–e. Fig. 3a shows that the maximum wicking height for the PAN/PDA nanofibrous membranes is obtained after a treatment time of 12 h. Dopamine modification of hydrophobic polymer membranes has been reported by Xi *et al.*[26] Jiang *et al.*[27] have demonstrated the mechanism of dopamine modification and

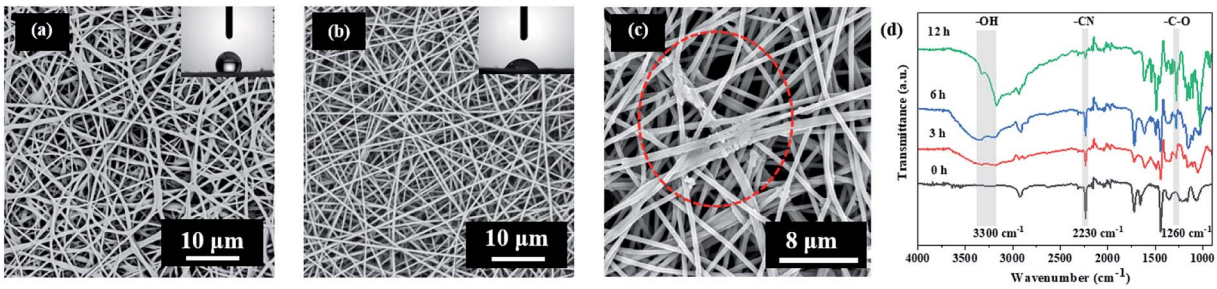

Fig. 2 SEM images of (a) TPU, (b) PAN, and (c) PAN/PDA. (d) FTIR spectra of PAN membranes with different PDA treatment times: 0, 3, 6, and 12 h.

concluded that the thickness of the deposited PDA layer increases with increasing reaction time. As a result, the PAN surface turns from hydrophilic to superhydrophilic because hydroxy and amino groups are successfully deposited on the PAN surface. Benefiting from the plasma and coating treatments, the fibrous membranes show excellent water-absorbing abilities and superhydrophilic properties. Fig. 3b shows a similar trend, where the water evaporation rate increases with an increase in the treatment time, with 12 h as the maximum. This can be attributed to the considerably wider water/air evaporation interface along the superhydrophilic membrane surface.[28,29] Water absorption and WCA investigations likewise show the improved hydrophilic performance of the fibrous membranes as the treatment time increases (Fig. 3c–e). Significantly, the water absorption times of the fibrous membranes are 5, 4, 4, and 1 s, respectively. Water droplets on the PAN/PDA fibrous membranes are clearly shown to be unstable and to quickly spread out in a short time. This finding indicates that the fibrous membranes are much more hydrophilic, and that the coating time plays a positive role in accelerating the wetting behavior and triggering water transport.

3.2 Directional water transport, moisture permeability, and breathability of the superhydrophilic fibrous membranes

To further study the water transport behaviors and comfort properties of the PAN/PDA superhydrophilic nanofibrous membranes, moisture management testing (MMT), air permeability, and WVT rates are studied to evaluate the functional membranes. The MMT results of the super-hydrophilic fibrous membranes are assessed after different PDA treatment times. Fig. 4a–d reveals no significant differences in the MMT results from PAN/PDA fibrous membranes with 0, 3, and 6 h coating treatment times, but a higher upward trend is shown when the PDA treatment time was 12 h. This result is likely attributed to the fact that PDA may not fully deposit on the film surface after a very short coating time period.[4] This finding is also supported by the wetting property results shown in Fig. 3a–e.

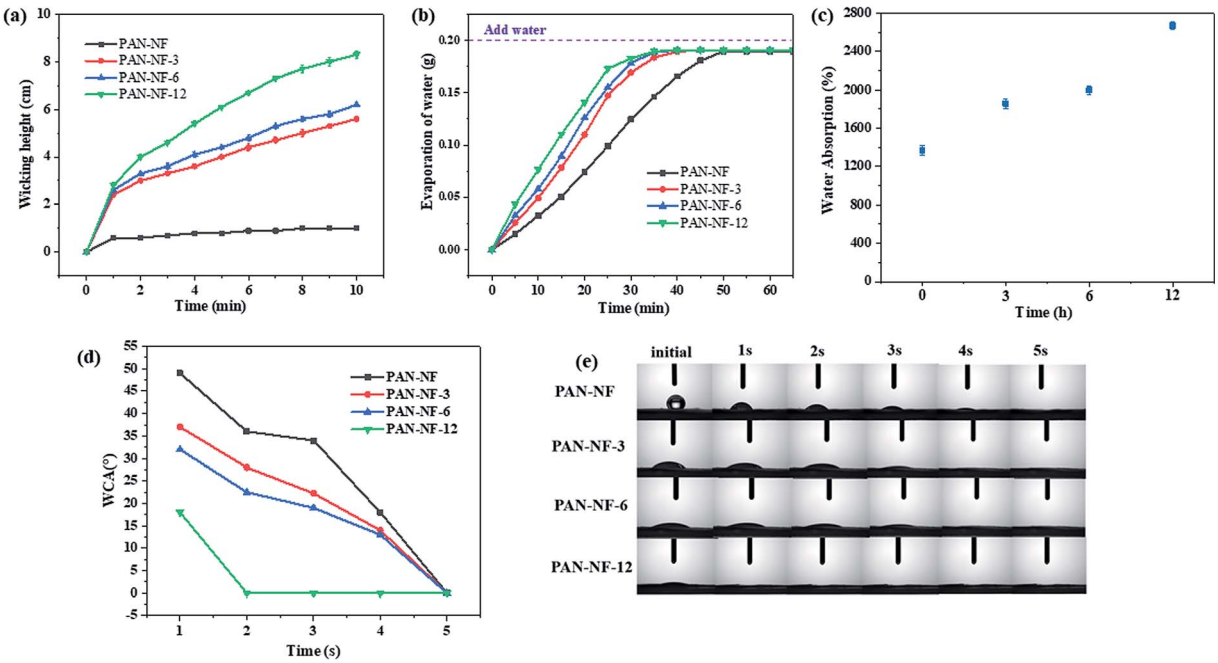

Fig. 3 The wetting behaviors of the PAN membranes with different PDA treatment times: 0, 3, 6, and 12 h. (a) The wicking height, (b) water evaporation rate, (c) water absorption, (d) WCA, and (e) apparent WCA of the corresponding fibrous membranes.

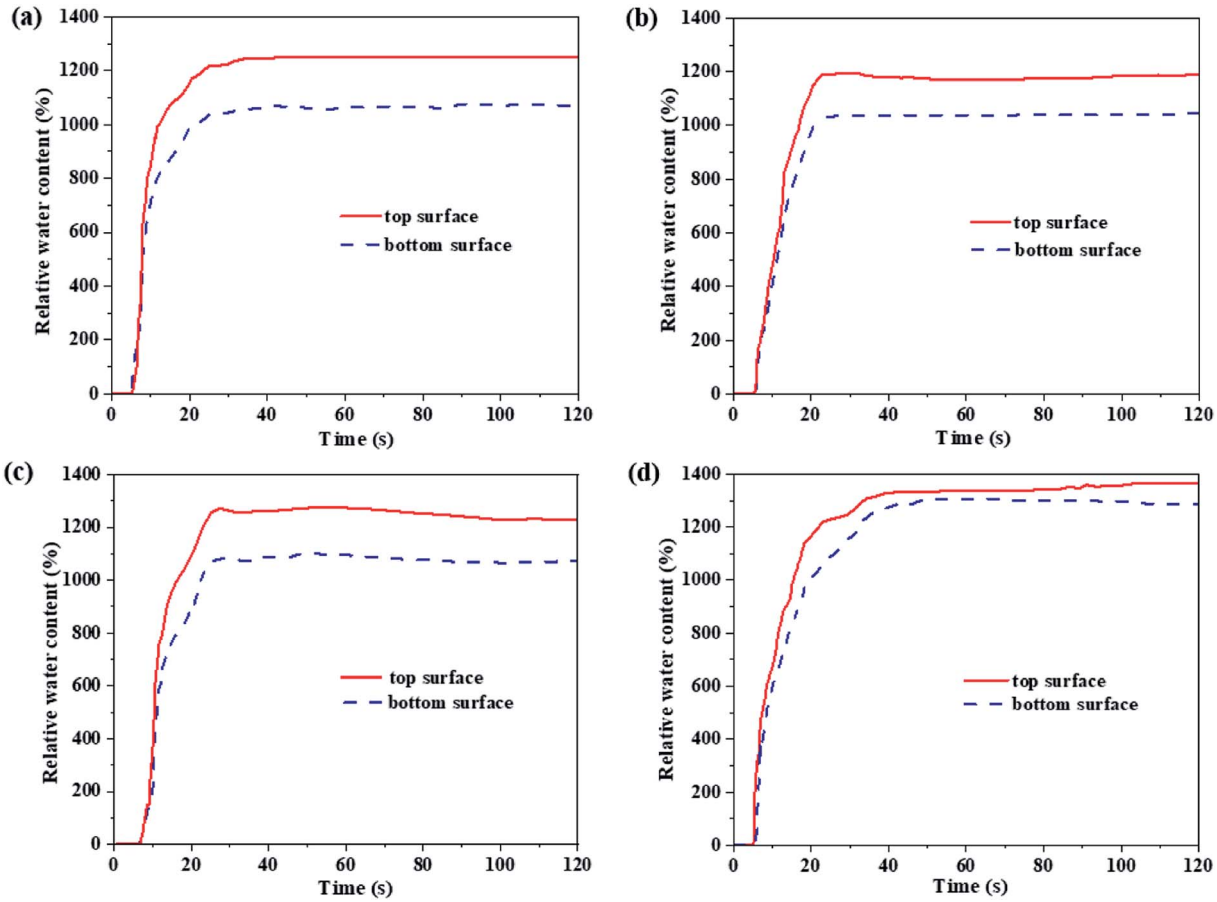

Fig. 4 The MMT results from PAN/PDA fibrous membranes after different treatment times: (a) 0 h, (b) 3 h, (c) 6 h, and (d) 12 h.

As mentioned earlier, the evaluation of the hydrophilic properties of porous nanofibers is crucial because the better the hydrophilic performance, the stronger the capillary effect will be, which will lead to improved water-wicking capabilities. However, from a functional perspective, moisture permeability and breathability are two other critical comfort-related properties of textiles. As illustrated in Fig. 5a, the air permeability results revealed no significant changes due to the low deposition of PDA over the spinning times used, corresponding to the SEM outcomes shown in Fig. 2b and c. Meanwhile, Fig. 5b shows that the WVT rate of the modified membrane samples increased from 8850 g m^{-2} d^{-1} to 9200 g m^{-2} d^{-1} with an increase in the treatment time. This outcome is attributed to the capability of the hydroxyl structures of PDA to effectively improve water solubility in PAN and the hydrophilicity of the coating.[30] Thus, PAN nanofibrous membranes with 12 h coating treatment are optimal candidates for further modification.

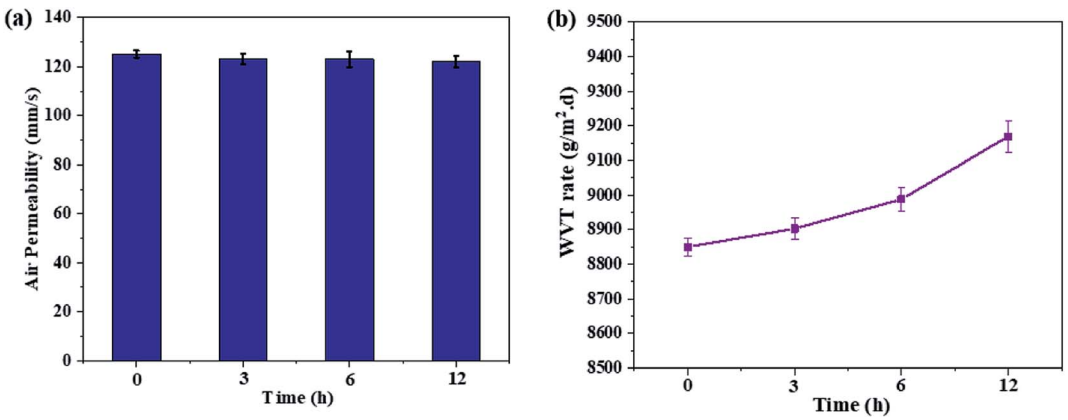

Fig. 5 (a) Air permeability and (b) WVT rates of the PAN/PDA fibrous membranes as the treatment time increases.

3.3 Directional water transport, moisture permeability, and breathability properties of the bi-layered Janus fibrous membranes

The MMT data from different bi-layered Janus fibrous membranes are shown in Fig. 6a–d. The solid and dashed lines represent the water content of the TPU surface (top side) and PAN/PDA surface (bottom side), respectively. During the MMT examination, 0.2 g of salted water was consistently dropped for 20 s on the TPU side and water movement in the bi-layered Janus fibrous membrane was observed for 120 s. Excellent moisture wicking performance can be obtained *via* tailoring the thicknesses of the top and bottom layers. Fig. 6a–d exhibits the water transport in bi-layered Janus fibrous membranes upon changing the bottom layer thickness, while maintaining the spinning time of the top layer (4 min). As illustrated in Fig. 6a, when the spinning time of the bottom layer is 15 min, the solid and dashed lines increase from the start and soon reach a steady-state value because the membrane is so thin that water can easily pass through the bi-layered Janus fibrous membrane. However, for bottom layer spinning times of 30 and 45 min, water can be effectively pushed into the pores in the top layer *via* capillary motion and pulled out by the hydrophilic bottom layer (Fig. 6b and c). This result can be attributed to the fairly large difference in hydrophilicity between the two layers, which can trigger directional water transport.[28] Furthermore, for a bottom layer with a spinning time of 30 min, the crossover of the two lines occurred within 30 s, whereas for a bottom layer with a spinning time of 45 min, the crossover occurred after 90 s, indicating that the former exhibits a faster water transport speed than the latter. Results for a bottom layer with a spinning time of 60 min are displayed in Fig. 6d. The water content in the top layer is higher than in the bottom layer, and no moisture wicking performance is shown due to the increase in the membrane thickness.[18] The water transport performances from different TPU spinning times are demonstrated in Fig. 6b, e and f. Increasing the TPU layer spinning time has an adverse effect on the water transport properties. In conclusion, a bi-layered Janus fibrous membrane with a highly thick hydrophobic layer can hinder water movement.[19] Therefore, the optimum electrospinning times for the bottom layer and top layer are 30 and 4 min, respectively.

As discussed above, the thickness, determined by the spinning time, and the wettability gradient are the main elements for improving the MMT results. The relationship between the bottom layer/top layer spinning time and directional water penetration is also illustrated in Fig. 7. The results in the figure display that when the TPU membrane spinning time is fixed at about 4 min, water can penetrate from the hydrophobic top side to the hydrophilic bottom side when the electrospinning times of the bottom layer are 30 and 45 min, respectively. However, if the electrospinning time of the bottom layer is above 45 min, then water droplets are absorbed by the bottom layer instead of penetrating across this layer because of the poor wettability gradient. Additionally, if the electrospinning time of the bottom layer is below 15 min, then no sufficient capillary force is provided by the super hydrophilic PAN/PDA membrane to overcome the resistance provided by the porous media channel lengths. This finding is further supported by the MMT results with and without PDA coating (Fig. 6b and g, respectively).

As seen in Fig. 6b, the TPU–PAN/PDA membrane can unidirectionally pump water from the hydrophobic layer to the superhydrophilic layer through an asymmetric wettability gradient. By contrast, water cannot be transported from the top hydrophobic surface to the bottom surface without PDA coating, thus showing the weaker capillary force of PAN. The MMT results were also compared for the two sides of the Janus membrane (Fig. 6b and h, respectively). For directional water transport Janus TPU-PDA/PAN fibrous membranes, the water content changes showed different trends on the two surfaces. When water was dropped on the hydrophilic surface (Fig. 6h), the water content clearly increased because the water feeding rate was higher than the water transport rate from the top to bottom layer in the Janus fibrous membranes during that time span. When the water feeding stopped, an apparent difference in the water content values of the two layers was observed. This phenomenon can be attributed to the pull–push effect of the Janus membrane. This result also conforms with the mechanism shown in Fig. 9.

To further observe the water transport properties, we evaluated the moisture permeability and breathability properties of the bi-layered Janus fibrous membranes. As shown in Fig. 8a and b, the air permeability and WVT rate decrease as the thickness of the bottom layer increases, showing a similar trend to the MMT results. According to the previous literature,[31,32] the porosity of fibrous membranes is commonly described *via* the following equation:

$$\text{Porosity} = \left(1 - \frac{m}{t \times S \times \rho}\right) \times 100\% \quad (1)$$

where m, t, and S are the mass, thickness, and area per unit of the measured membrane, respectively. In addition, ρ is the density of the polymer raw material. In terms of the Janus membranes, S and ρ are equal because the same materials are used. However, the mass and thickness values exhibited an increasing trend with different spinning times, with values of 4.338 and 4.942, and 5.118 and 5.572 g cm^{-1}, respectively. This variation trend indicates that the increase in the mass of the specimens was higher than the increase in thickness at a certain area per unit, resulting in a lower porosity value. Specifically, the porosity of the membranes decreased as the spinning time of the bottom layer increased. As a result, the air permeability decreased because of the decreased porosity (Fig. 8a). This conclusion is consistent with published papers.[30–33] However, the spinning time not only affected the air permeability, but it also influenced the WVT rate. The decreasing trends of the WVT rate and air permeability can be attributed to competition between capillary forces and resistance depending on the bottom layer thickness.[15] The resistance makes it harder for air or water to penetrate the membrane. The above results confirm that capillary forces and resistance force act against each other, and the resultant force determines the difficulty of penetration. When the bottom layer thickness is significantly decreased, the resistance is also decreased, while the capillary force remains

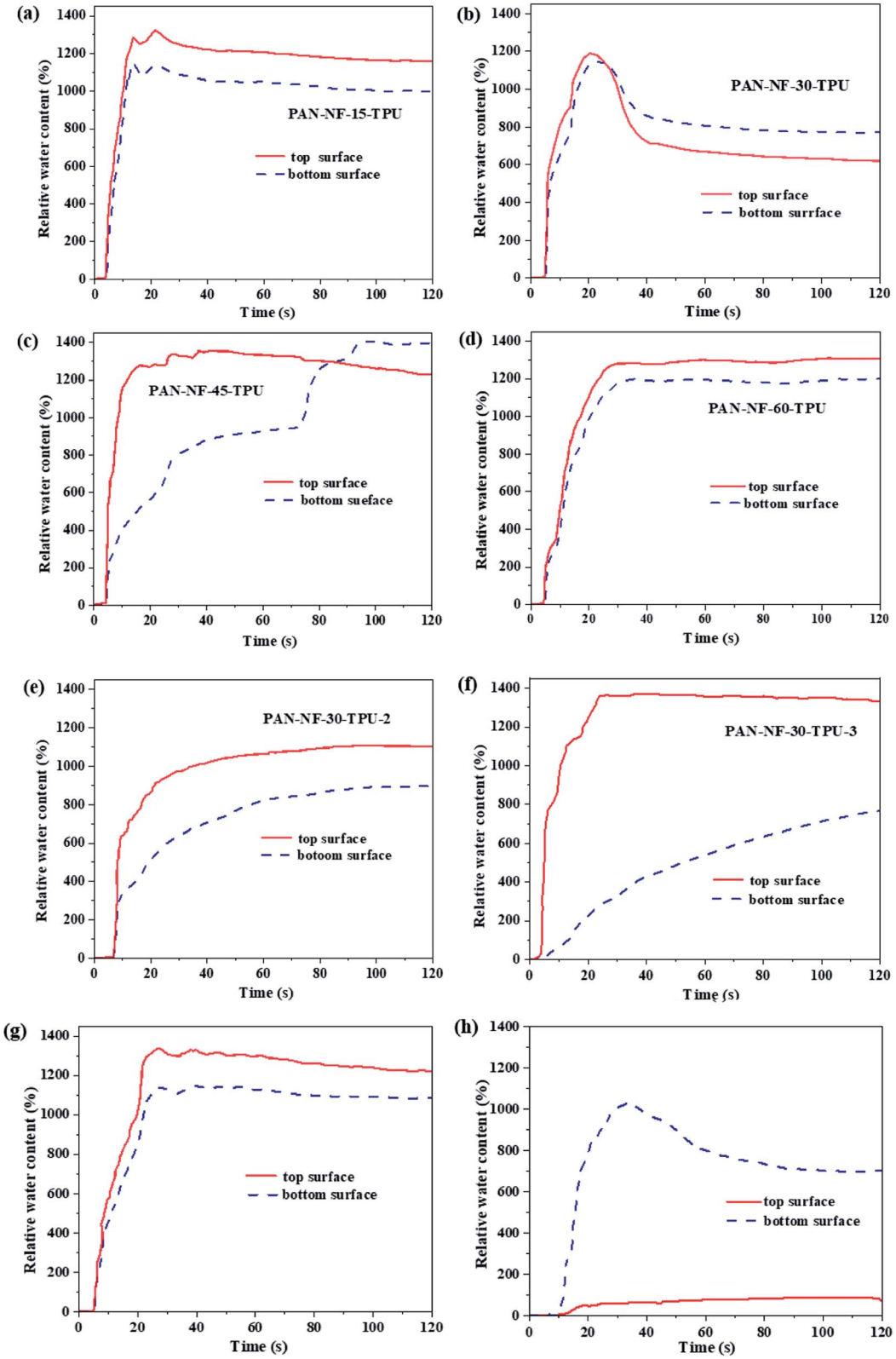

Fig. 6 MMT results from the bi-layered Janus fibrous membranes with respect to the electrospinning time used for the bottom layer: (a–d) 15, 30, 45, and 60 min, respectively; and the spinning time used for the top layer: (e and f) 8, and 12 min, respectively. (g) MMT results from a bi-layered Janus fibrous membrane without PDA-coating (the electrospinning times for the bottom layer and top layer are 30 and 4 min, respectively). The water is dropped onto the TPU surface. (h) MMT results from a bi-layered Janus fibrous membrane (the electrospinning times for the bottom layer and top layer are 30 and 4 min, respectively). The water is dropped on the PAN/PDA surface.

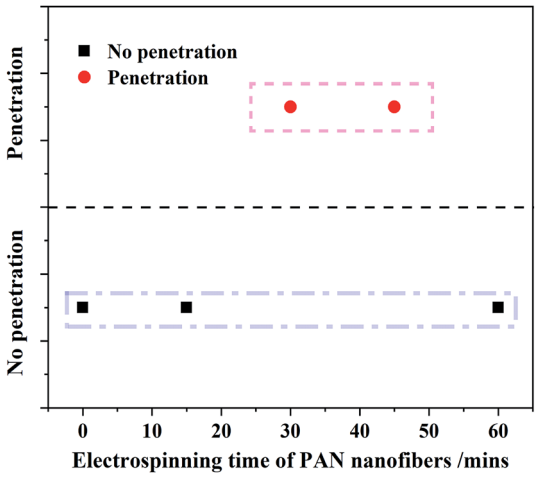

Fig. 7 The relationship between the bottom layer spinning time and the unidirectional water penetration.

constant during this process. Therefore, the breathability and moisture permeability can be tailed using the thickness gradient. Additionally, the perspiration of a normal adult in a state of motion is 1200–2000 g each day;[18] this is to say that a WVT rate of 2000 g m^{-2} d^{-1} can guarantee wearing comfort. A comparison of the performances of a commercial PU membrane, TPU/TPU-TBAC, and a TPU–PAN/PDA bi-layered Janus fibrous membrane is presented in Fig. 8c to evaluate the comfort performance. The figure clearly reveals that the bi-layered Janus fibrous membrane exhibits outstanding air permeability (100 mm s^{-1}) and a high WVT rate (9065 g m^{-2} d^{-1}), superior to those of the commercial fabric (0.302 mm s^{-1}, 1880 g m^{-2} d^{-1}) and the TPU/TPU-TBAC double layer membrane (1.16 mm s^{-1}, 2170 g m^{-2} d^{-1}). Consequently, the bi-layered Janus fibrous membrane exhibits excellent moisture-permeable and breathable performance and is suggested to be a promising candidate for all kinds of potential applications with respect to comfortable protective textiles.

The performances of bi-layered Janus membranes with and without PDA coating were compared as well. The membranes are denoted as TPU–PAN/PDA (with coating) and TPU–PAN (without coating). As seen in Table 1, when PDA is deposited onto the PAN membrane, the WVT rate increases slightly, confirming that better permeability performance occurs due to the relatively larger quantities of –OH groups on the PDA/PAN membrane. However, no large changes in air permeability were observed with and without the coating. Air permeability with and without the coating showed similar values.

3.4 The directional water transport mechanism in bi-layered Janus fibrous membranes

Generally, wettability and thickness gradients across bi-layered Janus fibrous membranes result in directional water transport behavior in water–air systems. Fig. 9a and b demonstrates the possible directional water transport mechanism in the bi-layered Janus fibrous membranes. As shown in Fig. 9a, from the hydrophobic side, with a fixed channel length, water can quickly spread along the bottom surface (the superhydrophilic layer) of the membrane because of competition between the hydrostatic pressure, wettability gradient, hydrophobic force, and capillary force. Among these factors, hydrostatic pressure (F_{HP}) results from the force of gravity, pushing water toward the hydrophilic layer.[15] The wettability gradient (F_{WG}) presents relatively higher numbers of inter-fiber gaps that the water can be pushed to move toward. However, hydrophobic force (F_{HF}) plays a positive role in preventing the downward penetration of water. Additionally, capillary force facilitates the spreading of water in all possible directions. When the water reaches the TPU interface, the phenomenon of water penetration through the hydrophobic layer into the hydrophilic layer will happen once F_{HP} and F_{WG} are larger than F_{HF}. On the other hand, when the

Table 1 A comparison between bi-layered Janus fibrous membranes with and without PDA coating

Performance	TPU–PAN	TPU–PAN/PDA
MMT test	No transport	One-way water-transport
WVT rate, g m^{-2} d^{-1}	8720	9065
Air permeability, mm s^{-1}	102	100

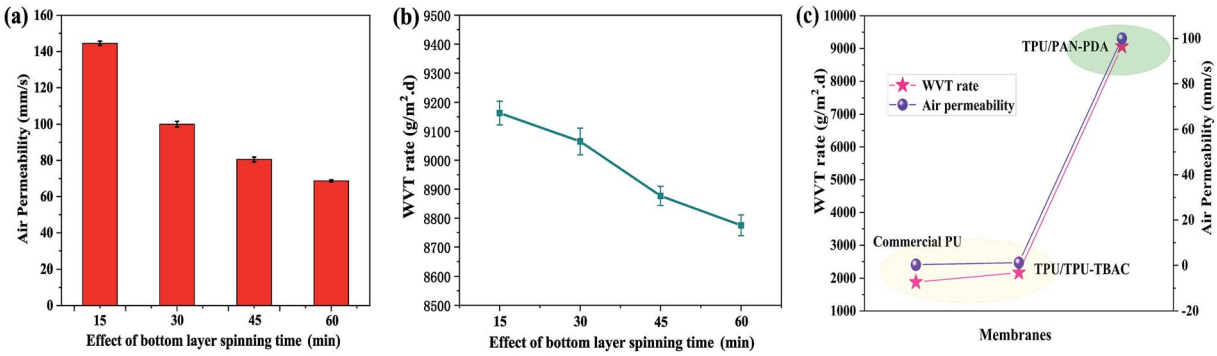

Fig. 8 (a) Air permeability and (b) WVT rates of bi-layered Janus fibrous membranes with different bottom layer spinning times. (c) WVT rate and air permeability data from a TPU–PAN/PDA bi-layered Janus fibrous membrane, a commercial PU membrane, and a double-layer TPU/TPU-TBAC membrane reported by Ju *et al.*.[18]

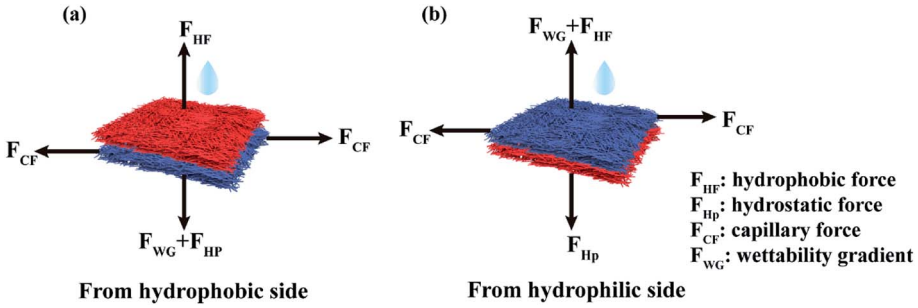

Fig. 9 The mechanism of unidirectional water transport on a bi-layered Janus fibrous membrane: (a) water drops onto the hydrophobic TPU side and penetrates the membrane immediately; (b) water drops onto the superhydrophilic PAN/PDA side and spreads rather than penetrates.

penetration depth reaches the thickness of the TPU film, water droplets wick into a superhydrophilic layer with capillary force (F_{CF}).[28,34] On the contrary, if a water droplet is dropped onto the hydrophilic side, F_{HP} will push the water to penetrate through the membrane, but F_{HF} offered by the TPU layer and F_{WG} between the two layers will hinder further water penetration. Meanwhile, F_{CF} offered by the hydrophilic layer ensures the quick spreading of water droplets, thus reducing the per unit F_{HP} area.[19] The results indicate that no directional liquid transport abilities exist from the hydrophilic to the hydrophobic layer.

4. Conclusions

In summary, bi-layered Janus fibrous membranes are prepared through the combination of PAN/PDA and TPU electrospun nanofibers. The nanofibers with superhydrophilic PAN/PDA are fabricated *via* plasma treatment and dip coating. The bi-layered Janus fibrous membranes, designed with different spinning times and coating treatment times, demonstrate that the thickness gradient plays an important role in the directional water transport, air permeability, and water vapor transmission rate. Moreover, the construction of a surface energy gradient introduces asymmetric wettability as another factor that pushes water from the hydrophobic TPU inner layer to the superhydrophilic PDA/PAN outer layer. As a result, the combination of a considered inner layer and outer layer leads to optimized directional water transport properties, outstanding moisture permeability of 9065 g m^{-2} d^{-1}, and distinct breathability of 100 mm s^{-1} (5.0 times higher than a commercial membrane). The results of this study prove that this is a valuable reference for the design and tailoring of three-dimension electrospun fibrous membranes with high breathability, high permeability, and directional water transport properties.

Author contributions

In this study, the concepts and design of experiments were supervised by Ching-Wen Lou and Jia-Horng Lin. Experiments and data processing were conducted by Yue Zhang and Ting-Ting Li. Text composition and analysis of results were performed by Yue Zhang and Ting-Ting Li. The experimental results were examined by Qi Lin, Fei Sun and Hai-Tao Ren. Dr Yue Zhang and Ting-Ting Li made equal contributions to the article.

Conflicts of interest

The authors declare no conflicts of interest.

Acknowledgements

This work is supported by the Natural Science Foundation of Tianjin (18JCQNJC03400), the Natural Science Foundation of Fujian (2018J01504, 2018J01505) and the National Natural Science Foundation of China (grant number 11702187). This study is also supported by the Opening Project of Green Dyeing and Finishing Engineering Research Center of Fujian University (2017001A, 2017001B, and 2017002B) and the Program for Innovative Research Teams in the University of Tianjin (TD13-5043).

References

1 Y. Liu, J. H. Xin and C. H. Choi, *Langmuir*, 2012, **28**(50), 17426–17434.
2 A. K. Yetisen, H. Qu, A. Manbachi, H. Butt, M. R. Dokmeci, J. P. Hinestroza, M. Skorobogatiy, A. Khademhosseini and S. H. Yun, *ACS Nano*, 2016, **10**(3), 3042.
3 Y. Dong, J. Kong, C. Mu, C. Zhao, N. L. Thomas and X. Lu, *Mater. Des.*, 2015, **88**, 82–87.
4 Y. Dong, J. Kong, S. L. Phua, C. Zhao, N. L. Thomas and X. Lu, *ACS Appl. Mater. Interfaces*, 2014, **6**(16), 14087–14095.
5 H. Zhou, H. Wang, H. Niu, C. Zeng, Y. Zhao, Z. Xu, S. Fu and T. Lin, *Adv. Mater. Interfaces*, 2016, **3**(17), 1600283.
6 H. Wang, X. Wang and T. Lin, *J. Nanosci. Nanotechnol.*, 2013, **13**(2), 839–842.
7 H. Wang, D. Jie, L. Dai, X. Wang and L. Tong, *J. Mater. Chem.*, 2010, **20**(37), 7938–7940.
8 A. A. Babar, X. Wang, N. Iqbal, J. Yu and B. Ding, *ACS Appl. Mater. Interfaces*, 2017, **4**(15), 1700062.
9 T. T. Li, M. Yan, W. Xu, B. C. Shiu, C. W. Lou and J. H. Lin, *Polymers*, 2018, **10**(10), 1167.
10 T. T. Li, Y. Zhong, M. Yan, W. Zhou, W. Xu, S. Y. Huang, F. Sun, C. W. Lou and J. H. Lin, *Nanomaterials*, 2019, **9**(5), 714.

11 J. E. Mates, T. M. Schutzius, J. Qin, D. E. Waldroup and C. M. Megaridis, *ACS Appl. Mater. Interfaces*, 2014, **6**(15), 12837–12843.
12 M. Rother, J. Barmettler, A. Reichmuth, J. V. Araujo, C. Rytka, O. Glaied, U. Pieles and N. Bruns, *Adv. Mater.*, 2016, **27**(42), 6620–6624.
13 M. Cao, J. Xiao, C. Yu, K. Li and L. Jiang, *Small*, 2015, **11**(34), 4379–4384.
14 X. Wang, Z. Huang, D. Miao, J. Zhao, J. Yu and B. Ding, *ACS Nano*, 2019, **13**(2), 1060–1070.
15 J. Wu, N. Wang, L. Wang, H. Dong, Y. Zhao and L. Jiang, *Soft Matter*, 2012, **8**(22), 5996.
16 J. Yang, H. N. Li, Z. X. Chen, A. He, Q. Z. Zhong and Z. K. Xu, *J. Mater. Chem. A*, 2019, **7**(13), 7907–7917.
17 Y. P. An, J. Yang, H. C. Yang, M. B. Wu and Z. K. Xu, *ACS Appl. Mater. Interfaces*, 2018, **10**(11), 9832–9840.
18 J. Ju, Z. Shi, N. Deng, Y. Liang, W. Kang and B. Cheng, *RSC Adv.*, 2017, **7**(51), 32155–32163.
19 A. A. Babar, D. Miao, N. Ali, J. Zhao, X. Wang, J. Yu and B. Ding, *ACS Appl. Mater. Interfaces*, 2018, **10**(26), 22866–22875.
20 H. Yang, Y. Lan, W. Zhu, W. Li, D. Xu, J. Cui and G. Li, *J. Mater. Chem.*, 2012, **22**(33), 16994–17001.
21 S. L. Phua, L. Yang, C. L. Toh, S. Huang, Z. Tsakadze, S. K. Lau and X. Lu, *ACS Appl. Mater. Interfaces*, 2012, **4**(9), 4571–4578.
22 H. Y. Son, J. H. Ryu, H. Lee and Y. S. Nam, *Macromol. Mater. Eng.*, 2013, **298**(5), 547–554.
23 S. M. Kang, I. You, W. K. Cho, H. K. Shon, T. G. Lee, I. S. Choi and H. Lee, *Angew. Chem., Int. Ed.*, 2010, **49**(49), 9401–9404.
24 H. Yang, Y. Lan, W. Zhu, W. Li, D. Xu, J. Cui, D. Shen and G. Li, *J. Mater. Chem.*, 2012, **22**(33), 16994–17001.
25 M. Muller and B. Kessler, *Langmuir*, 2011, **27**(20), 12499–12505.
26 Z.-Y. Xi, Y.-Y. Xu, L.-P. Zhu, Y. Wang and B.-K. Zhu, *J. Membr. Sci.*, 2009, **327**(1–2), 244–253.
27 J. Jiang, L. Zhu, L. Zhu, B. Zhu and Y. Xu, *Langmuir*, 2011, **27**(23), 14180–14187.
28 D. Miao, Z. Huang, X. Wang, J. Yu and B. Ding, *Small*, 2018, **14**(32), e1801527.
29 G. Havenith, P. Bröde, E. d. Hartog, K. Kuklane, I. Holmer, R. M. Rossi, M. Richards, B. Farnworth and X. Wang, *J. Appl. Physiol.*, 2013, **114**(6), 778–785.
30 F. Yang, Y. Li, X. Yu, G. Wu, X. Yin, J. Yu and B. Ding, *RSC Adv.*, 2016, **6**(90), 87820–87827.
31 Z. Wang, C. Zhao and Z. Pan, *J. Colloid Interface Sci.*, 2015, **441**, 121–129.
32 J. Wang, Y. Li, H. Tian, J. Sheng, J. Yu and B. Ding, *RSC Adv.*, 2014, **4**(105), 61068–61076.
33 L. Zhang, Y. Li, J. Yu and B. Ding, *RSC Adv.*, 2015, **5**(97), 79807–79814.
34 Y. Zhao, H. Wang, H. Zhou and T. Lin, *Small*, 2017, **13**(4), 1601070.